Enabling pseudo-ductility in geopolymer based glass-ceramics matrix composites by slurry dilution

Gilles Dusserre, Anaïs Farrugia, Thierry Cutard

Open Ceramics 7 (2021) 100156

Contents lists available at ScienceDirect

Open Ceramics

journal homepage: www.editorialmanager.com/oceram

Enabling pseudo-ductility in geopolymer based glass-ceramics matrix composites by slurry dilution

Gilles Dusserre *, Anaïs Farrugia, Thierry Cutard

Institut Clément Ader (ICA), Université de Toulouse, CNRS, IMT Mines Albi, INSA, ISAE-SUPAERO, UPS, Campus Jarlard, F-81013, Albi, France

ARTICLE INFO

Keywords:
Geopolymer-based composite
Carbon fibre
Pseudo-ductility

ABSTRACT

Carbon fibre reinforced composites with matrix consisting of porous glass-ceramics obtained by high temperature heat-treatment of geopolymer based material are studied. The matrix is obtained from a slurry. Several composites have been manufactured by in-laboratory stratification of pre-impregnated plies with slurries diluted at various rates. Slurry dilution changes the porosity and leads to pseudo-ductile behaviour of the composite. Dilution implies a drop of non-linearity stress threshold together with a slower decrease of the strength. An optimal dilution rate is evidenced, which exhibits high strength but lower non-linearity stress threshold, and then, a significant failure strain. The optimized prepreg material is compared with a reference composite processed by an industrial prepreg process. The origin of the pseudo-ductility is related to decohesion at the interface between tows and inter-tow matrix. RTM also provides a pseudo-ductile composite but with very low non-linearity stress threshold, in relation to poorly impregnated tows.

1. Introduction

The high specific properties of composite materials, specifically those reinforced with carbon fibres, are one of their most useful properties to lighten parts in many applications, including aeronautical structures. Fibre reinforced polymers are not suitable for long term exposure at high temperature (typically above 200 °C), whereas the cost of classical ceramic matrix composites is prohibitive at low temperature (typically below 1000 °C). Geopolymer based materials are light enough and able to withstand stresses in the intermediate temperature range [1], i.e. included between those two limits. Strength retention of 60% is expected at 800 °C [2]. Moreover, geopolymers can be used as matrix of composites by processes much less expensive than classical ceramic matrix composites. Most of the studies deal with particulate or short fibre reinforced geopolymers [1,3–5], mainly for construction. Only a few ones investigate carbon [6–10], SiC [11] or basalt [12] continuous fibres reinforced geopolymers. Recently, acid-based geopolymers have been proposed as alternatives compatible with oxide fibres [13].

Carbon fibres reinforced composites with a geopolymer based matrix exhibit excellent mechanical properties (tensile strength higher than 2.9 GPa and tensile modulus higher 250 GPa are reported in Ref. [10] for a unidirectional composite hardened at 75 °C). Their inorganic matrix makes them potential candidates to meet the requirements of structure parts at high temperature [4,5,8–10], and in particular, in the temperature range up to approximately 350 °C, in which the carbon fibres oxidation in air is slow. For safety reasons, in many applications, one of these requirements is the ability to withstand significant strains, leading brittle materials to be rejected. While metals overcome this limitation by plasticity at high temperature, ceramic matrix composites are based on weak components, that are able to deviate the cracks at the fibre/matrix interface [14], avoiding collective failure of the fibres inside a tow. A sudden failure of the part is thereby avoided, leading to a pseudo-ductile behaviour [15,16]. According to He et al. [8], the interphase between carbon fibres and geopolymer matrix is weak after exposure to temperature lower than 1000 °C, as shown by long fibre pull-out in fracture surfaces.

To achieve this behaviour, ceramics matrix composites are either based on weak fibre/matrix interfaces, or on a weak matrix. The former is usually obtained by a coating on the fibres, which is sometimes fugitive to control the interfacial porosity. For instance, this strategy has been proposed for geopolymers reinforced with PVA [17] or steel [18] short fibres, or alumina continuous fibres [19]. The latter strategy is more usual for porous oxide matrices [20] and requires a fine and evenly spread porosity [21,22].

The aim of this paper is to enable a pseudo-ductile behaviour in a geopolymer-based glass-ceramic composite reinforced with carbon

* Corresponding author. IMT Mines Albi - Institut Clément Ader, Campus Jarlard – route de Teillet, 81013, ALBI CT cedex 9, France.
E-mail address: gilles.dusserre@mines-albi.fr (G. Dusserre).

https://doi.org/10.1016/j.oceram.2021.100156
Received 31 March 2021; Received in revised form 21 June 2021; Accepted 23 June 2021
Available online 26 June 2021

Table 1
Composite properties.

Composite	Slurry dilution rate (wt.%)	Number of plies	Fibre volume fraction[a] (%)	Average ply thickness (mm)	Open porosity[b] (%)	Apparent density[b] ($g.cm^{-3}$)	True Density[b] ($g.cm^{-3}$)	Tensile elasticity modulus[c] (GPa)
PrepregREF	0	6	39 ± 2	0.29 ± 0.01	14.0 ± 0.7	1.66 ± 0.015	1.93 ± 0.020	76 ± 2
Prepreg0	0	6	38 ± 2	0.30 ± 0.01	18.4 ± 0.7	1.55 ± 0.014	1.89 ± 0.020	70 ± 1
Prepreg1	1	6	38 ± 2	0.30 ± 0.01	17.3 ± 0.7	1.57 ± 0.014	1.90 ± 0.020	70 ± 2
Prepreg2	2	6	38 ± 2	0.30 ± 0.01	18.9 ± 0.7	1.53 ± 0.014	1.89 ± 0.020	72 ± 1
Prepreg3	3	6	39 ± 2	0.29 ± 0.01	20.3 ± 0.7	1.51 ± 0.014	1.90 ± 0.021	68 ± 6
Prepreg4	4	6	40 ± 2	0.29 ± 0.01	22.9 ± 0.8	1.47 ± 0.014	1.91 ± 0.022	69 ± 2
Prepreg5	5	6	39 ± 2	0.29 ± 0.01	24.3 ± 0.8	1.46 ± 0.014	1.93 ± 0.022	65 ± 1
RTM3	3	7	39 ± 2	0.30 ± 0.01	25 ± 0.7	1.46 ± 0.020	1.95 ± 0.04	64 ± 5

[a] Estimated from composite thickness, number of plies, fabric areal density and fibre density.
[b] Estimated by hydrostatic weighing in air and distilled water of dry and wet samples (Sartorius LA3200DC balance, accuracy 0.002 g, equipped with Sartorius YDK 01 LP setup).
[c] Measured by tensile tests (cf. sections 2.5 and 3).

fibres, by using diluted slurry. The expected effects of slurry dilution are manifold. On the one hand, the matrix overall porosity may increase as a result of a lower solid volume fraction, but the porosity distribution can change as a result of a change in rheological behaviour [23]. On the other hand, matrix shrinkage may increase and stiffness decrease, which is expected to lead to a different state of initial cracking.

First, the dilution rate is optimized in order to promote pseudo-ductility without dramatic strength loss. This is achieved by in-laboratory process for pre-impregnated laminates. The material obtained is compared to a reference material obtained by an industrial process. Finally, thanks to dilution, liquid composite moulding is made possible. Prepreg and RTM composites processed with the optimized dilution rate are compared.

Analyses of microstructure and tensile behaviour are presented to understand the damage mechanisms, and provide new insights on how to achieve competitive pseudo-ductile materials.

2. Material and methods

2.1. Slurry

The matrix of the composites under study were manufactured from an industrial but non-commercial viscous slurry of density 1.75 g cm^{-3}. It is a geopolymer precursor of confidential composition, used for manufacturing parts made of pre-impregnated glass-ceramic matrix composite. The slurry consists in particles (size lower than 1 μm) in suspension in an aqueous solution of potassium silicate. The Si/Al ratio is much higher than unity.

Before processing the composite, the slurry is aged at −18 °C for several weeks. If the composite was not manufactured right after this period, the slurry was stored at a lower temperature to prevent any hardening. The diluted slurries are obtained by addition of 1 wt%, 2 wt%, 3 wt%, 4 wt% and 5 wt% (respectively 2.5, 5, 7.5, 10 and 12.5 vol%) of distilled water, with respect to the undiluted slurry weight. The mixing is made just before processing of the composite.

After hardening at low temperature, the slurry results in a porous geopolymer, which is heat treated at high temperature to provide the porous glass-ceramic matrix, of density 1.9 g cm^{-3} (Table 1).

25 mm length specimens of glass-ceramics were prepared by pouring slurry in an 8 mm diameter mould to measure the coefficient of thermal expansion of the matrix after hardening and heat treatment. The measurement was performed from room temperature up to 400 °C at a heating rate of 2 °C.min^{-1} using a Netzsch DIL 402 C dilatometer. The coefficient of thermal expansion of the glass-ceramic is 7.1 ± 0.7 10^{-6} K^{-1} between 100 and 400 °C.

2.2. Reinforcement

The reinforcement of all composites is a balanced 2/2 twill woven fabrics (200 g m^{-2}) of M40J-6 K high modulus carbon fibres (yield: 225 tex, filament diameter: 5 μm). According to the manufacturer datasheet, the tensile strength is 4410 MPa, the tensile modulus is 377 GPa, the density is 1.77 g cm^{-3} and the longitudinal coefficient of thermal expansion is −0.83 10^{-6} K^{-1}.

2.3. Composite processing

For all the composites, 6 or 7 plies (cf. Table 1) of woven fabrics were stacked by alternating the warp- and weft- orientation at 0° of the composites to get perfectly balanced laminates.

The composite plates were manufactured by three processes. The first one is an industrial stratification process of pre-impregnated plies. It is not suitable for diluted slurries and is used only to manufacture a reference material (referred to as "PrepregREF"). It is worth noting that the stratification studied in this paper is used for research only and is not related to any commercial material.

The second process is an in-laboratory stratification of pre-impregnated plies allowing the utilization of diluted slurries. It will be used to produce several materials for dilution rate optimization (referred to as "Prepregwt.%", where wt.%, the weight dilution rate, ranges between 0 and 5 wt %).

In both processes, the reinforcement is impregnated by simply immersing it in a slurry bath, but it is mechanised in the industrial process and by-hand in the in-laboratory process. 200 × 200 mm^2 plates were manufactured for each prepreg composite.

The third process is a resin transfer moulding involving the slurry with the optimal dilution rate, i.e. 3 wt%. A 150 × 400 mm^2 plate (referred to as "RTM3") was manufactured by injecting the slurry in a steel/PMMA mould, with a pressure drop of 3 bars between the injection gate and the vent, left at atmospheric pressure. A 2 mm thick spacer was used to ensure a fibre volume fraction of approximately 40%. To limit the hardening while processing, the slurry tank was placed in a cooling bath at 15 °C during injection in the mould at room temperature (approximately 20 °C).

After hardening at low temperature (60 °C for 12 h), the plates were demoulded and heat treated at high temperature (slightly higher than 600 °C, in accordance with the results of Tran et al. [9], which report an increase in mechanical properties after exposure to temperatures higher than 600 °C) under nitrogen to stabilize the porous glass-ceramic matrix.

Each plate was machined with water lubrication to provide the samples for morphological characterizations and the specimens for mechanical tests. The samples were dried at 80 °C for 24 h after machining. Table 1 summarizes the properties of the various composites. The so-called apparent and true densities differ by the open porosity volume, which is included in the material volume for the former and excluded for the latter. Both include closed porosity in the material volume. No significant difference is reported for true density, whereas the apparent density slightly decreases with increasing the dilution rate, as a result of a higher open porosity volume.

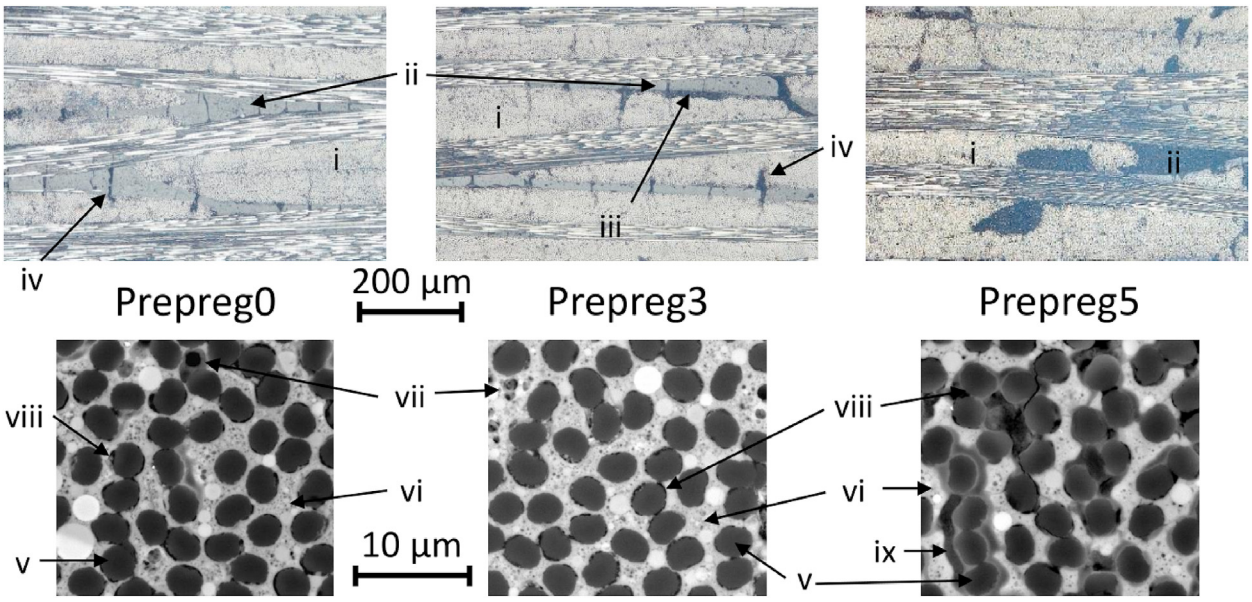

Fig. 1. Microstructure of in-laboratory prepared pre-impregnated materials from undiluted (Prepreg0), moderately (Prepreg3) and highly (Prepreg5) diluted slurry. i: tow; ii: inter-tow volume; iii. Decohesion; iv: crack; v: fibre; vi: intra-tow matrix; vii: pore; viii: interfacial porosity; ix: set of fibres locally unbonded.

2.4. Microstructure characterization

Polished cross-sections of each specimen were observed at the laminate scale with a numerical optical microscope (Keyence VHX-1000E), and at the fibre scale with a scanning electron microscope (FEI Nova-Nano SEM 450), without sample metallization thanks to the low vacuum mode (Gaseous Analytical Detector).

X-ray micro computed tomography (X-ray µ-CT) scans of samples of composites PrepregREF and Prepreg3 have been carried out. $2 \times 1.8 \times 0.6$ mm^3 samples have been analysed with 1.5 µm-edge voxels. The domains consisting of air are classified into pores and cracks depending on their aspect ratio, with a threshold set to 10. The items with an aspect ratio lower than 10 are classified as pores, whereas those with an aspect ratio higher than 10 are classified as cracks. This threshold value has been chosen based on the analysis of aspect ratio versus pore volume for the reference sample (PrepregREF). Indeed, pores larger than 10^3 µm^3 are clearly distributed into two distinct populations, a first one with aspect ratios spread between 1 and 10, and a second one with aspect ratios higher than 10 and following an increasing trend with volume. This rough classification focusses on large items and actually distinguishes macro-cracks (volume higher than 10^3 µm^3) from other pores (including micro-cracks of volume lower than 10^3 µm^3).

2.5. Tensile tests

200×15 mm^2 specimens were machined in the prepreg plates. 150×15 mm^2 specimens were machined in the RTM plate. The tensile specimens were equipped with 1.5 mm thick tapered aluminium alloy tabs bonded with a cyanoacrylate adhesive (50 mm long for prepreg, 37.5 mm long for RTM).

For each plate, three specimens were tested at room temperature. One preliminary test was performed on PrepregREF and Prepreg3 specimens at 350 °C to assess the suitability of the material in the intended temperature range.

The test procedure involves an incremental loading up to a stress increasing by 25 MPa, from 100 MPa up to failure, with unloading in-between.

All tests were performed in the 0° direction on a 250 kN MTS testing machine (15 kN range load cell) with hydraulic clamps, at a crosshead displacement rate of 1 mm min^{-1}. For the tests at 350 °C only the narrow section was heated in a furnace compatible with cold clamps.

The strain was measured with a 30 mm gauge length extensometer.

2.6. Dynamic elasticity modulus by impulse excitation of vibration

The elasticity modulus of PrepregREF and Prepreg3 composites were measured from room temperature up to 400 °C by impulse excitation of vibration [24]. 100×20 mm^2 specimens were tested on 50 mm spaced linear supports to enhance a low-frequency bending mode, at a heating/cooling rate of 2 K min^{-1}. A first heating/cooling cycle was performed up to 300 °C, followed by another one up to 350 °C, and a final one up to 400 °C.

3. Results and discussion

3.1. Optimal dilution rate for pseudo-ductile behaviour

The morphologic features of the six pre-impregnated composites obtained by in-laboratory process are displayed in the representative pictures of Fig. 1. For materials processed with undiluted slurry (Prepreg0), the inter-tows volumes (ii) are overall filled. Moderate dilution (Prepreg3) obviously increases the matrix shrinkage and leads to decohesion (iii) at the interface between the impregnated tows and the inter-tow volumes. In both cases (Prepreg0 and Prepreg3), the matrix in the inter-tow volumes exhibits evenly spaced cracks (iv) oriented through the thickness. For materials processed with a moderately diluted slurry (Prepreg3), these cracks seem to propagate into the tows (i) more likely. The inter-tows volumes of materials obtained with highly diluted slurry (Prepreg5) seem to be unfilled, but it is possibly due to the removal of non-adherent and cracked matrix during grinding and polishing. The tows seem to be only marginally cracked.

Inside the tows, the matrix microstructure seems to be unchanged by a moderate dilution (Prepreg0 and Prepreg3, Fig. 1), with a similar intra-tow matrix porosity (vi and vii). These materials are characterized by a very discontinuous fibre/matrix interface (viii), with, though, a surrounding of the fibres (v) by the matrix (vi). For high dilution rates, this interfacial porosity seems to coalesce, resulting in sets of several fibres locally unbonded (ix). A non-uniform loading of the fibre inside a tow is thus expected.

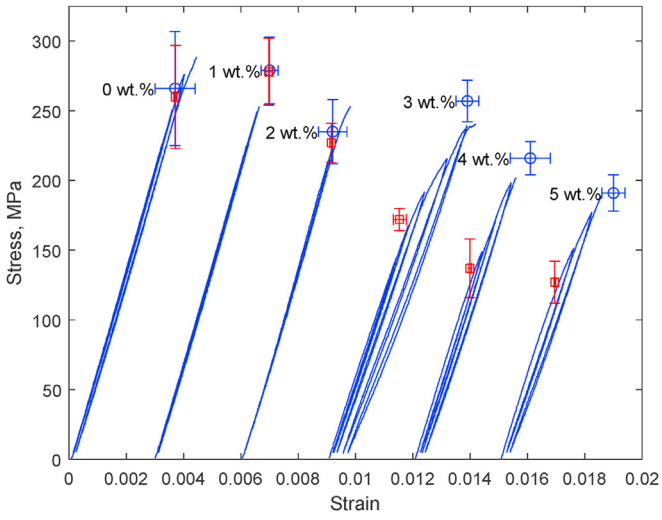

Fig. 2. Tensile behaviour of in-laboratory prepreg materials obtained with X wt.% diluted slurries (X, the weight dilution rate, ranges from 0 to 5). The curves are shifted horizontally of 0.003 × X. Blue circles indicate the tensile strength and failure strain. Red squares indicate the non-linearity stress threshold and the corresponding strain assuming the average modulus (horizontal error bars materialize the standard deviation on modulus). Preference for colour: online only. (For interpretation of the references to colour in this figure legend, the reader is referred to the Web version of this article.)

The tensile stress-strain curves of the in-laboratory prepared pre-impregnated composites are displayed in Fig. 2. The materials obtained with low diluted slurries, up to 2 wt%, are unsurprisingly brittle, since both components (carbon fibres and porous glass-ceramic matrix) are brittle. Very little differences are noticed between Prepreg0, Prepreg1 and Pregreg2 composites, with a slight decrease of strength for the latest. For slurry dilution rates of 3 wt% and higher, the onset of non-linear behaviour is significantly lower than the failure stress, in relation with a pseudo-ductile non-linear behaviour. However, the strength of Prepreg3 composite remains high, whereas it slightly decreases by further increasing the dilution rate.

The non-linearity is characterized by a damage elastic behaviour, as evidenced by the decrease of the tangent modulus with the successive loadings. For instance, Prepreg3 loading modulus decreases of 4% after being subjected to a tensile stress of 200 MPa, 10% after a stress of 225 MPa and 14% after a stress of 250 MPa. Moreover, a bilinear behaviour is evidenced in damaged materials, especially while unloading. For instance, the Prepreg3 unloading modulus after being subjected to 225 MPa and 250 MPa is 14% higher above 150 MPa than below. Under high stresses, the tangent modulus of damaged material is even slightly higher than the initial value for undamaged material. This behaviour is typical of tow straightening under tensile loading in damaged CMCs reinforced with woven fabrics, as detailed in Ref. [25] and reported in Refs. [26–29].

The pseudo-ductility of materials obtained with moderately to highly diluted slurries can thus be related to the non-completely filled inter-tow volumes, as illustrated in Fig. 1 (ii), in relation with higher matrix shrinkage, through the following hypothetic scenario. The resulting gaps allow the tows to straighten, as described in Ref. [25]. The shear stresses inside the tows resulting from fibre straightening lead to a progressive damage of the intra-tow matrix. This damage obviously depends on intrinsic matrix and interface strength, and is therefore sensitive to matrix porosity, also changed by dilution. For moderate dilution rates, the gaps are thin decohesions (iii, Fig. 1) at the interface between the tow and the intra-tow matrix. Tension results in the closure of these cracks, which stops the straightening of the adjacent tows, before the failure. This further allows to withstand higher loads. As a result, a significant pseudo-ductile behaviour is promoted with only a reduced strength loss as counterpart.

For high dilution rates, the gaps are too thick or the intra-tows matrix not tough enough to limit the straightening of the tows, that fail prematurely. The overall behaviour is therefore pseudo-ductile, but the composite strength is strongly reduced. Another scenario is conceivable, similar to the mechanism reported in Ref. [29], that involves a transverse

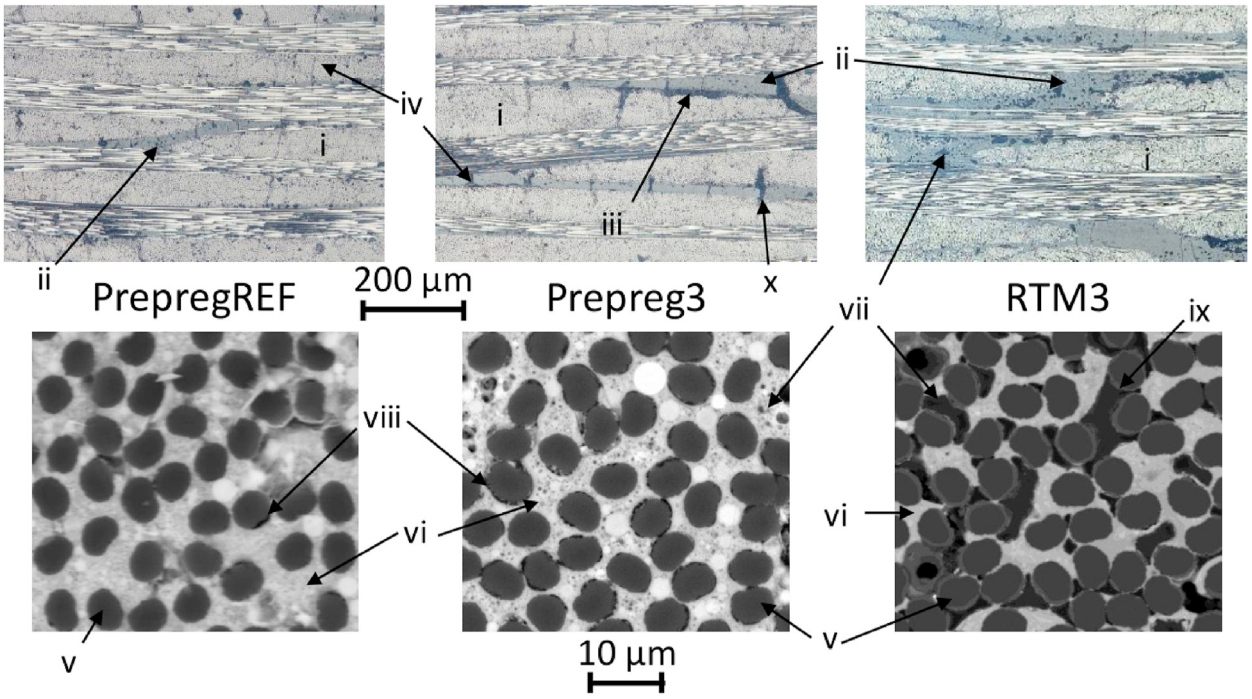

Fig. 3. Microstructure of industrial pre-impregnated material (PrepregREF, undiluted slurry), in-laboratory prepared pre-impregnated material (Prepreg3, 3 wt% diluted slurry) and in-laboratory prepared RTM material (RTM3, 3 wt% diluted slurry). i: tow; ii: inter-tow volume; iii. Decohesion; iv: crack; v: fibre; vi: intra-tow matrix; vii: pore; viii: interfacial porosity; ix: set of fibres locally unbonded; x: crack crossing the interface between a tow and inter-tow volume.

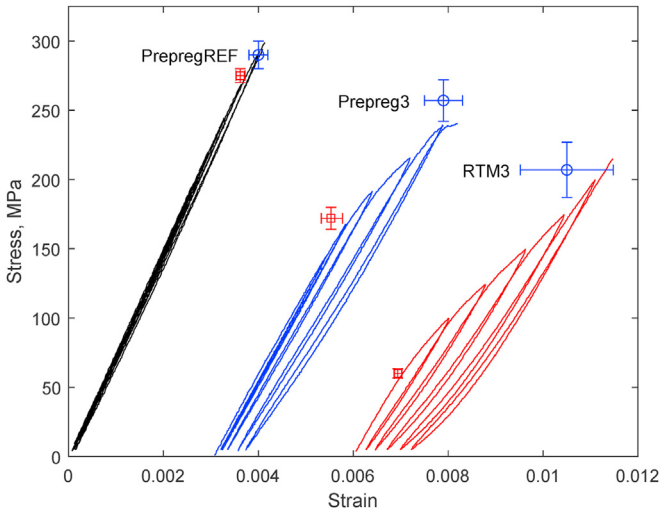

Fig. 4. Tensile behaviour of industrial pre-impregnated material (PrepregREF, undiluted slurry), in-laboratory prepared pre-impregnated material (Prepreg3, 3 wt% diluted slurry) and in-laboratory prepared RTM material (RTM3, 3 wt% diluted slurry). Prepreg3 and RTM3 curves are shifted horizontally of 0.003 and 0.006 respectively. Blue circles indicate the tensile strength and failure strain. Red squares indicate the non-linearity stress threshold and the corresponding strain assuming the average modulus (horizontal error bars materialize the standard deviation on modulus). Preference for colour: online only. (For interpretation of the references to colour in this figure legend, the reader is referred to the Web version of this article.)

failure of the very porous inter-tows matrix, compressed between the straightening tows.

As a conclusion of section 3.1, 3 wt% diluted slurry leads to pseudo-ductile materials that can be considered as optimized, i.e. the strain at break is significantly increased and the strength is not strongly affected. The stress at first damage is however significantly reduced. In section 3.2, this pseudo-ductile laboratory composite is compared to the reference material obtained by an industrial process without dilution.

3.2. *Damage mechanisms in brittle and pseudo-ductile composites*

3.2.1. *Behaviour at room temperature*

Compared to materials obtained by in-laboratory stratification process, the material obtained by the industrial process is much less porous (Table 1). As a result of a reduced matrix shrinkage, the inter-tow volumes (ii) are filled with weakly cracked matrix (iv, Fig. 3, PrepregREF). Inside the tows, the matrix exhibits a lower and finer porosity (vi and vii), leading to a less discontinuous fibre/matrix interface (viii). This results in a higher and less scattered strength and a significantly higher tensile elasticity modulus, 76 GPa for PrepregREF and 68 GPa for Prepreg3 (Table 1 and Fig. 4). The brittle failure of PrepregREF is characterized by a propagation of cracks across the tows without deviation at the fibre/matrix interface (Fig. 5, PrepregREF). A very different behaviour is displayed in Fig. 5 for Prepreg3. The fibres fracture seems less correlated and the fibres are separated, indicating a complex crack propagation path transverse to the tows.

X-ray μ-CT scans for PrepregREF and Prepreg3 composites are summarized in Fig. 6. The overall porosity volume fraction is 0.62% for PrepregREF and 7.62% for Prepreg3. The analysed volume is too low to be representative of the whole material. That's the reason of the difference with the porosity values reported in Table 1. However, the analysis confirms that Prepreg3 material is much more porous than the reference material (PrepregREF).

X-ray μ-CT scans provide an insight onto pore aspect ratio and volume distribution. Air domains of aspect ratio lower than 10 are classified as pores, those with an aspect ratio higher than 10 are classified as cracks. Fig. 6.a shows that the pore volume distribution is very similar in both samples. The pores volume fraction is 0.55% in PrepregREF and 0.32% in Prepreg3. This difference is not significant in view of the sample volume. A surprising difference is the absence of pores of volume lower than 270 μm^3 (8 μm equivalent diameter) in the Prepreg3 sample. At first sight it seems to be contradictory with the pores shown in Fig. 1 (Prepreg3). However, it may indicate that the pores are interconnected, as illustrated in Fig. 7. In PrepregREF sample, pores as small as 1.9 μm of equivalent diameter (volume of 3.4 μm^3) are reported, which indicate that the pores are unconnected (within the resolution of the scans).

The cracks volume fraction is very low in PrepregREF sample, 0.07%. It is strongly higher, 7.3%, in the Prepreg3 sample. Fig. 6.b evidences that this large difference is not specific to some ranges of crack volume (except a few very large cracks whose number is not representative), and concerns all the cracks volume distribution. This is illustrated by the onsets of Fig. 6.b and consistent with the pictures of Fig. 3 (PrepregREF and Prepreg3).

Compared to PrepregREF material, Prepreg3 composite is characterized by four main morphological features.

a. A partial decohesion between tows and inter-tow matrix
b. Important initial damages with evenly spaced cracks perpendicular to the fibres. Some of them propagate through tows and inter-tow matrix
c. A finely discontinuous fibre/matrix interface (but with still a surrounding of the fibres by the matrix).
d. An interconnected intra-tow porosity

In view of the brittle behaviour of Prepreg0, Prepreg1 and Prepreg2, which share the morphological characteristics (b) to (d) with Prepreg3, it can be concluded that pseudo-ductility in such composites is mainly

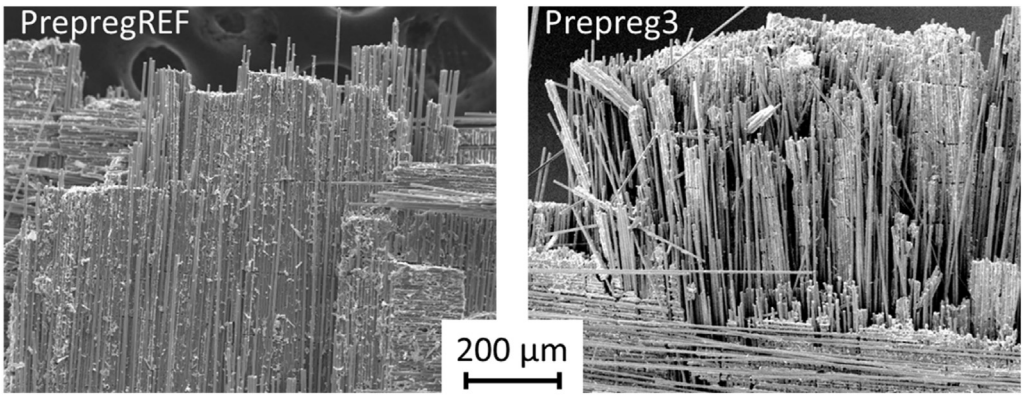

Fig. 5. Tensile fracture surfaces of brittle industrial pre-impregnated material (PrepregREF, undiluted slurry) and pseudo-ductile in-laboratory prepared pre-impregnated material (Prepreg3, 3 wt% diluted slurry).

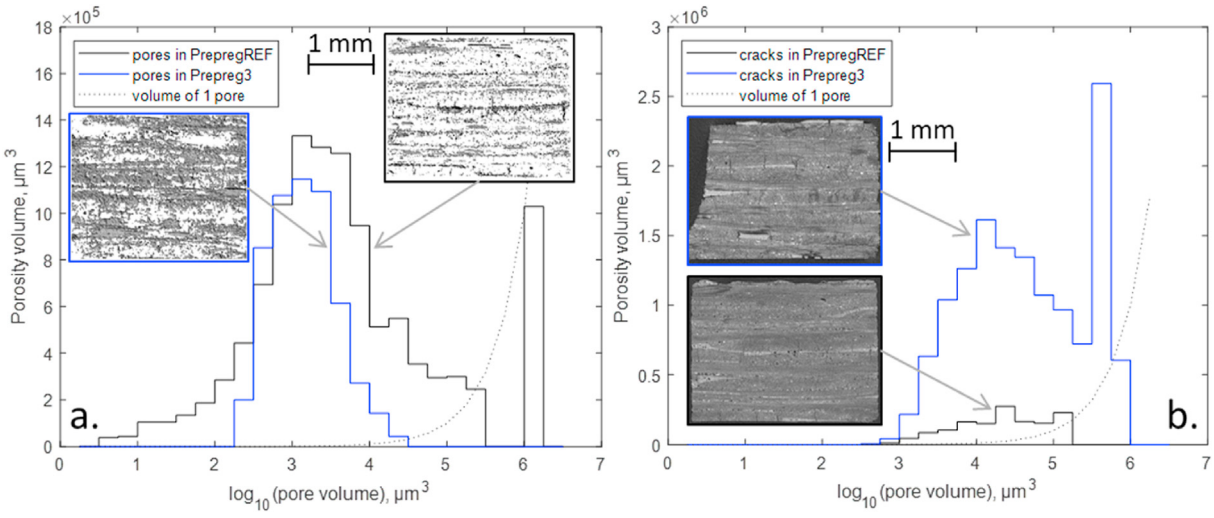

Fig. 6. Porosity distribution in brittle industrial pre-impregnated material (PrepregREF, undiluted slurry) and pseudo-ductile in-laboratory prepared pre-impregnated material (Prepreg3, 3 wt% diluted slurry): total porosity volume in a range of individual (a.) pore (aspect ratio lower than 10) or (b.) crack (aspect ratio higher than 10) volume. Insets in a. illustrate the whole porosity across the thickness of the samples. Insets in b. display a cross-section of the sample. The volume of one pore of the interval is plotted in dotted lines. Preference for colour: online only. (For interpretation of the references to colour in this figure legend, the reader is referred to the Web version of this article.)

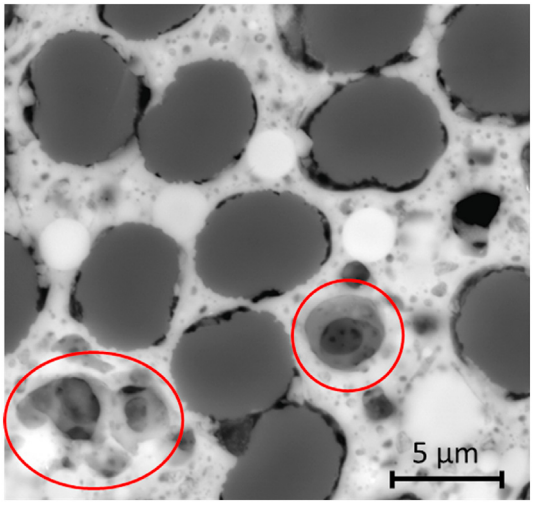

Fig. 7. SEM micrographs illustrating the interconnected porosity (red ellipses) in composite Prepreg3. Preference for colour: online only. (For interpretation of the references to colour in this figure legend, the reader is referred to the Web version of this article.)

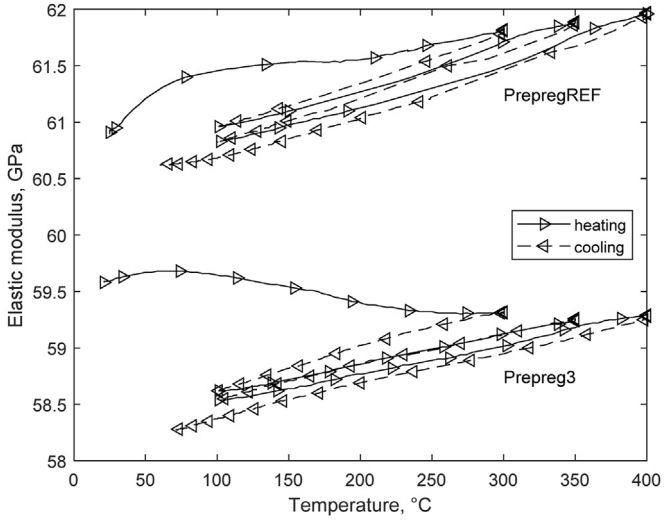

Fig. 8. Dynamic flexural modulus of industrial pre-impregnated material (PrepregREF, undiluted slurry) and in-laboratory prepared pre-impregnated material (Prepreg3, 3 wt% diluted slurry) between room temperature and 400 °C.

related to the characteristic (a). Indeed, even if cracks seem to be able to propagate across the interface between the tow and the inter-tow matrix (cf. Fig. 3, Prepreg3, x), it cannot propagate across the whole thickness because of such partial decohesion (cf. Fig. 3, Prepreg3, iii). As explained in section 3.1, the damage at the matrix and the fibre/matrix interface inside the tows is progressive thanks to the straightening of the tows, which is made possible by these decohesions. Failure of the inter-tow matrix may also occur, as described in Ref. [29], but more lately, when the tows are straightened enough to close the decohesions.

However, pseudo-ductility can be achieved, together with acceptable strength, only if the inter-tow matrix is still partially adherent to the tow, i.e. decohesion at the interface between tows and inter-tow matrix is not complete, which requires a fine tuning of the porosity induced by the in-laboratory prepreg process. If the porosity exceeds an acceptable value (corresponding to a dilution rate close to 3 wt%, i.e. an open porosity of 20% according to Table 1), the interconnected porosity coalesces and large pores arise, that lead to a lack of surrounding of the fibres by the matrix and therefore to sets of several fibres unbonded. This turns out to be detrimental to the strength of the composite.

3.2.2. *Effect of temperature on the mechanical behaviour*

The dynamic flexural modulus of materials PrepregREF and Prepreg3 are plotted in Fig. 8 as a function of temperature up to 400 °C. During the first heating, the very non-linear curves are related to the drying of the specimen. The subsequent cooling and heating steps show a more linear behaviour characterized by a slight increase of the modulus with temperature and a decrease of modulus with the previous exposure to higher temperature. This is an effect of the mismatch of thermal expansion between fibre and matrix. Indeed, matrix thermal expansion implies the closure of the cracks and a slight increase of the modulus. However, the cracks are likely to slowly propagate during cooling and a lower elasticity modulus is obtained while re-heating because of the increase of damages.

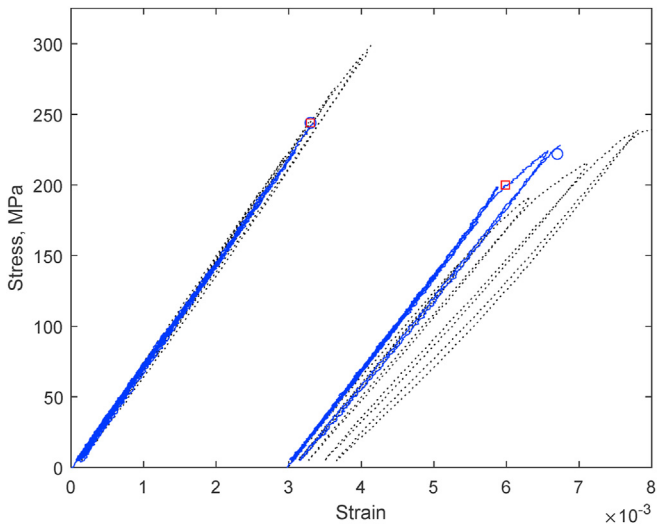

Fig. 9. Tensile behaviour at 350 °C of industrial pre-impregnated material (PrepregREF, undiluted slurry) and in-laboratory prepared pre-impregnated material (Prepreg3, 3 wt% diluted slurry). The curves at room temperature for the materials are plotted as dotted lines. Red squares indicate the non-linearity stress threshold and the corresponding strain. Preference for colour: online only. (For interpretation of the references to colour in this figure legend, the reader is referred to the Web version of this article.)

Fig. 8 shows that the behaviour of the material is not significantly affected by temperature, at least at short time range, except slight damages related to heating/cooling cycles. This is confirmed in Fig. 9, which displays the tensile behaviour at 350 °C of PrepregREF and Prepreg3 composites. This paper is not devoted to a thorough characterization of the high temperature behaviour. However, these preliminary results provide some information to better understand the damage mechanisms. Neither very important difference between the behaviour at room temperature and at 350 °C is evidenced. In particular, the modulus is unchanged. However a higher stress at the onset of non-linearity seems to be noteworthy (200 MPa at 350 °C instead of 172 ± 8 MPa at room temperature). This result is still to be confirmed but it may indicate that the first damage is sensitive to the mismatch of thermal expansion between fibre and matrix, i.e. they are located inside the tows, which corroborates the mechanism explained previously. Heating may lead to crack closure or contact pressure increase between fibre and matrix and the stress required to damage the interface may increase. Similar effects are reported in [26], with an increase of the strength at high temperature, explained by the mismatch of thermal expansion between fibre and matrix, and by a decrease of the residual stresses resulting from a temperature closer to the manufacturing temperature.

3.3. Comparison of pre-impregnated and RTM composites

The composite elaborated by RTM with the optimal dilution rate, 3 wt %, also behaves as a pseudo-ductile material, as shown by Fig. 4 (RTM3). Its properties reported in Table 1 and its strength are very close to those of Prepreg5, processed with a highly diluted slurry (5 wt%). However, its stress at the onset of non-linearity, as well as its morphological characteristics are very different. Indeed, the former is 60 ± 3.3 MPa instead of 127 ± 15 MPa for Prepreg5 and 172 ± 8 MPa for Prepreg3. The tensile behaviour of the damaged RTM3 material is bilinear, as reported for Prepreg3, but the slope change occurs for very low stresses, close to 60 MPa (150 MPa for Prepreg3).

This confirms that porosity morphology has an influence on the onset of pseudo-ductility.

Fig. 3 (RTM3) shows that the inter-tow volumes are filled with uncracked matrix (neither through the thickness, nor at the boundaries of the tows), contrarily to the matrix of the material obtained by in-laboratory stratification process. Pores of quite large dimensions (about 0.05 mm) are dispersed in the inter-tow volumes, which is not the case in the other materials (except some large bubbles of a tenth of mm), but there is no decohesion at the interface between the tow and the inter-tow matrix. The pseudo-ductile behaviour may be related to another microscopic feature.

The intra-tow matrix has a very different microstructure than observed previously in the pre-impregnated materials. As seen for Prepreg 5 (Fig. 1), pores have coalesced, leading to sets of fibres to remain locally unbonded by the matrix (Fig. 3, RTM3). Very narrow matrix necks are evidenced between some fibres. Moreover, the matrix doesn't exhibit the fine interconnected porosity of pre-impregnated materials. An apparently dense matrix is observed inside the tows, but it doesn't surround all the fibres. Local stress concentration would lead the brittle and narrow necks to fail at a quite low macroscopic stress. The pseudo-ductile behaviour would be related to the straightening of the fibres, made possible by the collapse of unevenly consolidated tows, instead of the spaces available at the interface between the tows and the inter-tow matrix.

4. Conclusions

Slurry dilution allows to manufacture pseudo-ductile composites by pre-impregnated plies stratification. Dilution obviously increases porosity and matrix shrinkage. Intra-tow matrix porosity increases first homogeneously and lead to interconnected pores. For high dilution rates, the pores coalesce and sets of fibres remain locally unbonded by the matrix.

Due to shrinkage, for low dilution rates, the inter-tow matrix exhibits cracks but still fills the intra-tow volumes. For higher dilution rates, decohesion between tows and inter-tow matrix starts, up to a complete uncoupling (at least after grinding and polishing).

As a result, an optimal dilution rate can be achieved close to 3 wt%, which provides an intra-tow matrix that completely surrounds the fibres and exhibits an evenly distributed interconnected porosity. The decohesion at the interface between tows and inter-tow matrix is mainly thin cracks that allow the tows to straighten (with a damage of the intra-tow matrix), but only in a limited range. This is thought to be the main feature of pseudo-ductility in the prepreg composites under study.

RTM process with diluted slurry also provides a pseudo-ductile behaviour but with very different features. First, an uncracked and more porous matrix fully fills the inter-tow volumes. The intra-tow matrix exhibits a very non-uniform porosity, with dense necks bonding some fibres while sets of fibres are not surrounded by the matrix.

The prepreg pseudo-ductile material has much better mechanical properties than RTM one and seems to be a good compromise between pseudo-ductility and high stress at the onset of non-linearity. A preliminary tensile test at high temperature suggests that increasing the stress at the onset of non-linearity is possible by strengthening the fibre-matrix interface.

Declaration of interests

The authors declare that they have no known competing financial interests or personal relationships that could have appeared to influence the work reported in this paper.

Acknowledgment

Part of this work was carried out in the framework of the collaborative project COMPTINN′ funded by OSEO-DGCIS within the field of the ASTech and Aerospace valley competitiveness clusters.

References

[1] N. Ranjbar, M. Zhang, Fiber-reinforced geopolymer composites: a review, Cement Concr. Compos. 107 (2020) 103498.

[2] A. Poulesquen, F. Frizon, D. Lambertin, Rheological behavior of alkali-activated metakaolin during geopolymerization, in: F. Bart, C. Cau-di-Coumes, F. Frizon, S. Lorente (Eds.), Cement-Based Materials for Nuclear Waste Storage, Springer, New York, 2012, pp. 225–238.

[3] R.A. Ribeiro, M.G. Ribeiro, W.M. Kriven, A review of particle- and fiber-reinforced metakaolin-based geopolymer composites, J. Ceram. Sci. Technol. 8 (2017) 307–322, https://doi.org/10.4416/JCST2017-00048.

[4] V.F.F. Barbosa, K.J.D. MacKenzie, Thermal behaviour of inorganic geopolymers and composites derived from sodium polysialate, Mater. Res. Bull. 38 (2003) 319–331.

[5] P. Behera, V. Baheti, J. Militky, P. Louda, Elevated temperature properties of basalt microfibril filled geopolymer composites, Construct. Build. Mater. 163 (2018) 850–860.

[6] D.H. Tran, et al., Effect of curing temperature on flexural properties of silica-based geopolymer carbon reinforced composite, JAMMME 37 (2009) 492–497.

[7] S. Yan, et al., Effect of fiber content on the microstructure and mechanical properties of carbon fiber felt reinforced geopolymer composites, Ceram. Int. 42 (2006) 7837–7843.

[8] P. He, D. Jia, T. Lin, M. Wang, Y. Zhou, Effects of high-temperature heat treatment on the mechanical properties of unidirectional carbon fiber reinforced geopolymer composites, Ceram. Int. 36 (2010) 1447–1453.

[9] D.H. Tran, P. Louda, D. Kroisova, O. Bortnovsky, T.X. Nguyen, New generation of geopolymer composite for fire-resistance, in: P. Tesinova (Ed.), Advances in Composite Materials – Analysis of Natural and Man-Made Materials, InTech, 2011, pp. 73–92.

[10] J. Zhao, M. Liebscher, A. Michel, D. Junger, A.C. Constâncio Trindade, F. de Andrade Silva, V. Mechtcherine, Development and testing of fast curing, mineral-impregnated carbon fiber (MCF) reinforcements based on metakaolin-made geopolymers, Cement Concr. Compos. 116 (2021) 103898.

[11] P. He, et al., SIC fiber reinforced geopolymer composites, part 2 : continuous SiC fiber, Ceram. Int. 42 (2016) 12239–12245.

[12] M. Welter, M. Schmücker, K.J.D. MacKenzie, Evolution of the fibre-matrix interactions in basalt-fibre-reinforced geopolymer-matrix composites after heating, J. Ceram. Sci. Tech. 6 (2015) 17–24.

[13] V. Mathivet, J. Jouin, S. Rossignol, M.H. Ritti, M. Parlier, Composites Synthesized with Acid-Based Geopolymers, HTCMC 10th, Book of abstracts, Bordeaux, France, Sep 2019 abstract n°1859.

[14] M.-Y. He, J.W. Hutchinson, Crack deflection at an interface between dissimilar elastic materials, Int. J. Solid Struct. 25 (1989) 1053–1067.

[15] Sanjeev Kumar, Bensingh Dhas, Debasish Roy, Emergence of pseudo-ductility in laminated ceramic composites, Compos. Struct. 204 (2018) 664–676.

[16] Gérald Camus, Modelling of the mechanical behavior and damage processes of fibrous ceramic matrix composites: application to a 2-D SiC/SiC, Int. J. Solid Struct. 37 (2000) 919–942.

[17] Behzad Nematollahi, Jishen Qiu, En-Hua Yang, Jay Sanjayan, Microscale investigation of fiber-matrix interface properties of strain-hardening geopolymer composite, Ceram. Int. 43 (2017) 15616–15625.

[18] Navid Ranjbar, Mehdi Mehrali, Mohammad Mehrali, U. Johnson Alengaram, Mohd Zamin Jumaat, High tensile strength fly ash based geopolymer composite using copper coated micro steel fiber, Construct. Build. Mater. 112 (2016) 629–638.

[19] Patrick R. Jackson, Donald W. Radford, Effect of initial cure time on toughness of geopolymer matrix composites, Ceram. Int. 43 (2017) 9884–9890.

[20] F.W. Zok, C.G. Levi, Mechanical properties of porous-matrix ceramic composites, Adv. Eng. Mater. 3 (2001) 15–23.

[21] W.-C. Tu, F.F. Lange, A.G. Evans, Concept for a damage-tolerant ceramic composite with “strong” interfaces, J. Am. Ceram. Soc. 79 (1996) 417–424.

[22] C.G. Levi, J.Y. Yang, B.J. Dalgleish, F.W. Zok, A.G. Evans, Processing and performance of an all-oxide ceramic composite, J. Am. Ceram. Soc. 81 (1998) 2077–2086.

[23] G. Dusserre, A. Farrugia, T. Cutard, Rheology of a geopolymer precursor aqueous suspension during ageing, Int. J. Appl. Ceram. Technol. 17 (2020) 1802–1810.

[24] ASTM International, ASTM E 1876 : 2009 - Standard Test Method for Dynamics Young's Modulus, Shear Modulus, and Poisson's Ratio by Impulse Excitation of Vibration, 2009.

[25] S.F. Shuler, J.W. Holmes, X. Wu, Influence of loading frequency on the room-temperature fatigue of a carbon-fiber/SiC-matrix composite, J. Am. Ceram. Soc. 76 (1993) 2327–2336.

[26] Y. Shi, F. Kessel, M. Friess, N. Jain, K. Tushtev, Characterization and modelling of tensile properties of continuous fiber reinforced C/C-SiC composite at high temperatures, J. Eur. Ceram. Soc. 41 (2021) 3061–3071.

[27] E. Vanswijgenhoven, J. Holmes, M. Wevers, A. Szweda, The influence of loading frequency on the high-temperature fatigue behaviour of a Nicalon-fabric-reinforced polymer-derived ceramic-matrix composite, Scripta Mater. 38 (1998) 1781–1788.

[28] J.M. Staelher, S. Mall, L.P. Zawada, Frequency dependence of high-cycle fatigue behaviour of CVI C/SiC at room temperature, Compos. Sci. Technol. 63 (2003) 2121–2131.

[29] P. Reynaud, A. Dalmaz, C. Tallaron, D. Rouby, G. Fantozzi, Apparent stiffening of ceramic-matrix composites induced by cyclic fatigue, J. Eur. Ceram. Soc. 18 (1998) 1827–1833.